

Kinematics of a musculoskeletal model using inertial and magnetic measurement units

Koning B.H.W.^{1,2}, Van der Krogt M.M.^{1,3}, Baten C.T.M.², Koopman H.F.J.M.¹

¹Laboratory of Biomechanical Engineering, University of Twente, Enschede, The Netherlands

²Roessingh Research and Development, Enschede, The Netherlands

³Dept. of Rehabilitation Medicine, Research Institute MOVE, VU University Medical Center, Amsterdam, The Netherlands

Inertial and magnetic measurement units; global optimization; joint constraints; kinematic driver

1. INTRODUCTION

Inertial and magnetic measurement units (IMMUs, [1]) are becoming a serious candidate for human movement analysis in clinical settings or sports [2, 3]. They are (relatively) cheap, quick and not bothered by typical drawbacks of optical motion capturing devices, such as occlusion of markers and restriction to a lab environment. Combined with instrumented force shoes [4], it enables musculoskeletal modelling based on ambulatory measurements. However, currently available commercial musculoskeletal modelling programs, such as the AnyBody Modeling System (AMS, [5]), only provide integrated routines to drive these models using measured optical markers. We therefore developed a new IMMU driver for the AMS, which we validated against default marker drivers. For this purpose we compared the right hip kinematics of three simulations where we used marker drivers, IMMU drivers and a combination of both. We also compared simulated right thigh IMMU sensor signals (accelerometer and gyroscope) of each simulation to those measured by the real sensor. The results show to be promising and sensor signals can be reproduced accurately. However, before application of the new IMMU drivers important issues regarding sensor to segment calibration, appropriate joint constraints and handling of soft tissue artefacts (STAs) need to be solved.

2. METHODS

Definition of the IMMU driver

The IMMU driver is included in the AnyBody model in a way similar to the currently available marker drivers, by defining each IMMU twice (Figure 1). First, a *model IMMU* segment is rigidly attached to a default position on the model, with its orientation with respect to segment determined by functional calibration [2]. Secondly, a *real IMMU* segment is linked to the model IMMU using a hinge joint. Its orientation in global space is determined by fusion of the sensor signals outside the AMS [1]. Next, a three dimensional variable is used to define the rotation between the model and real IMMU using the attitude ‘vector’ defined by Woltring, [6];

$$AV = \alpha \mathbf{u}. \quad (1)$$

Where \mathbf{u} defines the instantaneous axis of rotation in the model IMMU frame (direction cosines) and α the angle of rotation around this axis (helical angle).

Global optimization and sensor signal reproduction

The variables are implemented as soft constraints, which results in an over-determinate (bio)mechanical system. The motion of the complete model in terms of the time-dependent generalised coordinates $\mathbf{q}(t)$ is determined by minimization of these soft constraints, $\Psi(\mathbf{q}, t)$, whilst fulfilling the hard constraints defined by joint constraints in the biomechanical model, $\Phi(\mathbf{q}, t)$ [5].

$$\begin{aligned} \min_{\mathbf{q}} G(\Psi(\mathbf{q}, t)) \\ \text{s. t. } \Phi(\mathbf{q}, t). \end{aligned} \quad (2)$$

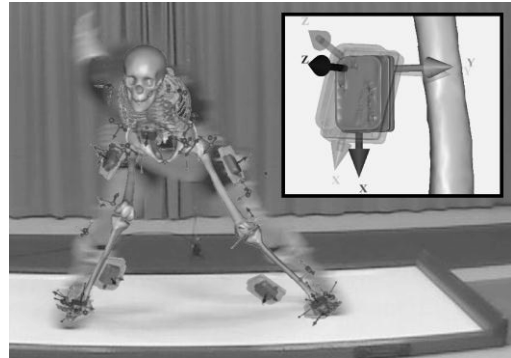


Figure 1 Screen capture of the slideboard experiment with an overlay of the AnyBody model. Top right shows the real (transparent) and model IMMU on the right thigh segment, including the local reference frames. Note the rotation around the sensor Y-axis.

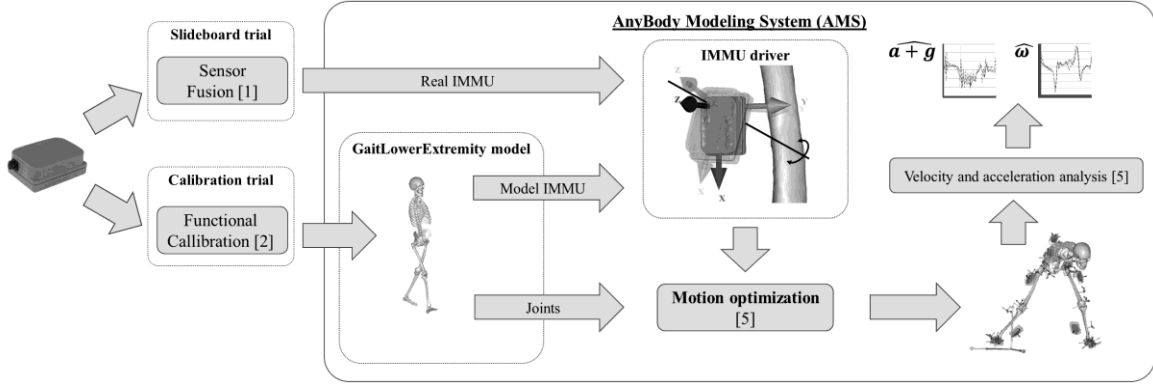


Figure 2 Optimization scheme for the new IMMU driver. Segment calibration determines the orientation of each model IMMU with respect to its segment of the GaitLowerExtremity model and fusion of the sensor signals during the slideboard experiment determines the orientation of the real IMMU in global space. The difference in orientation between the model and real IMMUs are minimized for each time step during the motion optimization, whilst completely fulfilling the joint constraints. After solving the optimization for the complete trial, model IMMU accelerometer ($\alpha + g$) and gyroscope signals (ω) are calculating using the Karush-Kuhn-Tucker conditions.

Once the generalised coordinates are known for the complete trial, the Karush-Kuhn-Tucker (KKT) are applied to calculate the model IMMU sensor signals [5]. The whole optimization scheme and reconstruction of the IMMU sensor signals is illustrated in Figure 2.

Weight functions

The objective function is a weighted least-square, with a constant weight.

$$G(\Psi(q, t)) = \Psi(q, t)^T W \Psi(q, t) \quad (3)$$

In this abstract the weight of the IMMU sensors was based on setting a constraint violation of 3 degrees equal to a 0.5 cm marker constraint violation, resulting in an IMMU weight of 0.095 m/rad. For the simulation without using IMMU drivers, the weight function was set to zero, so the IMMU driver constraint violations and sensor signals could still be determined for the marker driven model.

Experiments

Kinematics were obtained using synchronized measurements with IMMUs (Xsens Technologies, Enschede, The Netherlands) and optical markers (Vicon, Oxford, United Kingdom) of a subject using a slideboard, which is a land training setup for speed skating. The IMMU to segment calibration was performed using the direction of the accelerometer signal during a neutral upright pose to define the vertical segment axis and the gyroscope signal (angular velocities) during a sagittal plane squat to determine the mediolateral segment axis. For the simulations we used a slightly adapted version of the GaitLowerExtremity model from the AnyBody Modeling System repository (AnyBody Technology A/S, Aalborg, Denmark), having 15 joint constraints; Pelvis/Trunk (ball), Hip (ball), Knee (hinge), Ankle (hinge) and Subtalar (hinge). Three simulation were performed; one using marker drivers, one using the new IMMU drivers and one using both drivers simultaneously. The pelvis was fixed to the global reference frame when using IMMU drivers, due to the lack of position information.

3. RESULTS

Figure 3 shows the right hip kinematics of one motion cycle (3.68s) for the three simulations. Hip flexion angles showed an offset between simulations that included IMMU drivers and the one without, and also the hip external rotation angles were more similar for simulation including the IMMU drivers. The hip abduction angles showed opposite results; these were more similar for simulations including marker drivers.

Figure 4 shows the simulated and measured sensor signals around (gyroscope) and in the direction of (accelerometer) the right thigh sensor Z-axis. This axis happened to be approximately aligned with the segment's mediolateral segment axis (see Figure 1), i.e. the main direction of the sideways slideboard movement and the segment rotation axis associated with hip flexion. All simulated gyroscope signals (Figure 4, left) represented the measured gyroscope signals well, except where the simulated signals using marker drivers deviate from the measured signals (0 to 10% and 52 to 70%). The accelerometer signals (Figure 4, right) simulated using IMMU drivers showed the biggest deviations from the measured signal and also a more high frequent behaviour. Which in some cases showed great resemblance to the measured accelerometer signal (0-5% and 30-35%). Best correspondence with the measured accelerometer signals was achieved for simulations that included both drivers.

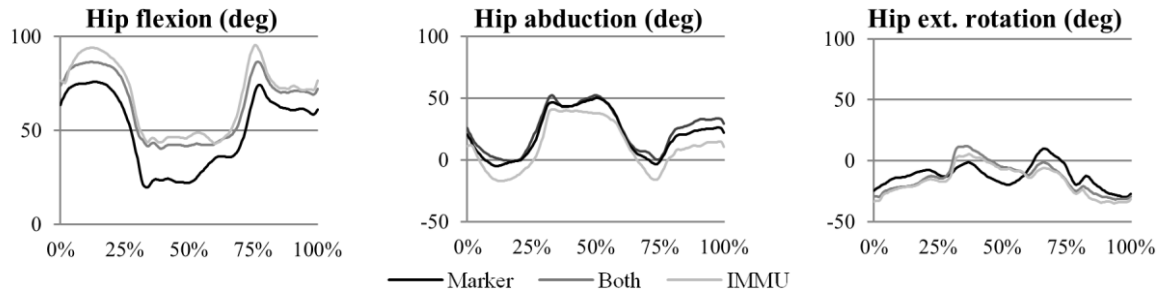


Figure 3 Simulated hip, knee and ankle flexion angles using marker, IMMU and both drivers. The cycle started with the moment where the right foot hit the side of the slideboard (0%). The subject prepared for push-off by flexing the right leg, followed by the actual push-off from 20 to 31%. The right leg was nearly extended while the subject slid to the left and was being pulled in after the left foot hit the board (52%). During the left leg push-off (starting at 70%) the right leg was pushed forward and lateral, and finally placed back on the slideboard (82%). After which it slid to the right, without fully extending the leg, until it hit the board again (100%).

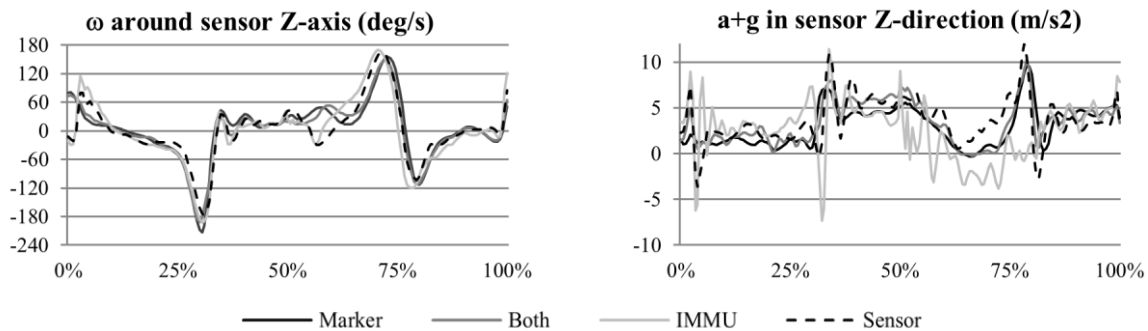


Figure 4 Simulated right thigh sensor kinematics for simulations using marker, IMMU and both drivers, compared to the measured sensor signals (Real). LEFT: gyroscope signals, RIGHT: accelerometer signals.

4. DISCUSSION

The great similarities between the right hip flexion and external rotation angles for simulations that included IMMU drivers and abduction angles for simulations that included marker drivers (Figure 3) were caused by two effects. The first was a methodological difference between the IMMU and marker drivers; for marker drivers a rotation around the segment long axis, compared to a similar rotation around one of the other axes, results in a smaller marker constraint violation due to the short distance of the markers to the segment long axis. There is no such direction dependency in the IMMU driver, implicitly making the IMMU driver more dominant for rotations along the long axes and small segments such as the feet.

The second and more important cause was a difference in segment calibration, which for the marker driven model was implicitly defined by the model marker placement. Figure 5 shows the soft constraint violations of the right thigh IMMU driver during the calibration trial. The offsets around the sensors local X and Z-axis (M_x , M_y), and thus the helical angle ($M\alpha$), when using marker drivers illustrated the difference between the model IMMU functional calibration and implicit marker calibration in the neutral position (10 to 12.5s). However, it lowered during the squat movement which is a more relevant pose for the slideboard trial. Optimization of both model marker and IMMU placement on the biomechanical model could reduce this calibration offset.

When using the IMMU drivers the constraint violation logically started at zero, as this was the starting pose for the functional calibration. But the constraint violation increased during the squat by rotating along the Y-axis (I_y), which was approximately aligned with the segment's frontal axis. This was caused by motion artefacts during the squat and the model's joint constraints in the knee. The latter actually prevented the squat movement to be simulated completely in the sagittal plane, which was the assumption for the used segment calibration procedure, unless the model's anatomical knee axis was normal to this plane. This illustrates the incorrectness of the used knee joint constraints.

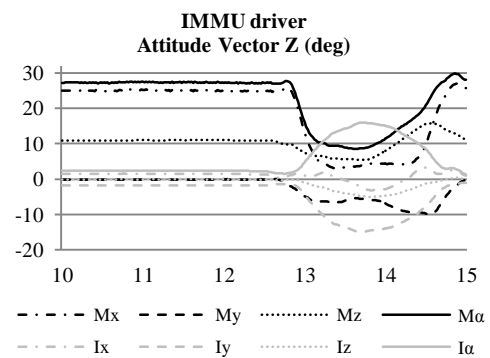


Figure 5 Values of the right thigh IMMU driver soft constraint violations for the marker (M) and IMMU driven (I) simulation of the calibration trial; a neutral upright body position, followed by a squat. It shows the x/y/z attitude vector elements and helical angle, α , of (1).

The early peaks (0-5%) in both measured sensor signals of Figure 4 were the result of soft tissue artefacts (STAs) caused by hitting the side of the board, from which it can be concluded that the IMMU driver is more sensitive to STAs. One reason is the limited amount of IMMU drivers, compared to the marker drivers. So the degree of model over-determinacy is much bigger when using marker drivers, effectively filtering the simulation output. This also explains some of the higher frequency content of the simulated accelerometer signals when using only IMMU drivers. However, this hypothesis needs validation.

The greater similarity between the simulated and measured gyroscope signals for the simulation using IMMU drivers was expected, as the real IMMU orientation was based on integration of the gyroscopic signal and the only deviation between the real and model IMMU was caused by the joint constraints. Direct comparison of the accelerometer signals was limited by the difference in segment calibration, inducing a different gravitational component, and also because pelvic fixation when using IMMU drivers eliminated an important component of the linear acceleration. Both causes for accelerometer signal difference were eliminated by removing the model estimate of the gravitational component and including one marker driver at the pelvis in the simulation using IMMU drivers (Figure 6). The resulting net linear acceleration estimates showed no further offset. So it can be concluded that the possible bias caused by the (a priori) estimated position of the model IMMU on the segment, and its effect on the net acceleration ($a = \omega^2 r$), was negligible.

In conclusion, we have developed a new kinematic driver for the AnyBody Modeling System that uses the orientation estimate obtained from sensor fusion of 3D accelerometers, gyroscopes and magnetometers. After the motion optimization, model sensor signals were calculated and compared to the measured sensor signals. It was even possible to further investigate the individual sensor signals by decomposition of the accelerometer signal. Results showed promising, but also illustrated the need for a more accurate sensor to segment calibration using a more task and pose specific method or minimization of the difference between simulated and measured sensor signals. Additionally, negative effects of the joint constraints and STAs on the resulting motion should be evaluated. Some effects of STAs could be reduced by using multiple sensors for each segment or by lowering the sensor weight functions for segments and directions where STAs are expected. To enable analysis of the accelerometer signals and improve the model's global accelerations (and thus inertial forces) global position constraints are necessary, such as GPS or UWB measurements, estimates of the centre of mass [4] or by implementing boundary conditions during contact with the environment.

5. ACKNOWLEDGMENTS

The Fusion3D project is funded by: Sterktes in de Regio, Vitaal Gelderland 2008 and Economische Innovatie Overijssel.

6. REFERENCES

- [1] D. Roetenberg, 2006. "Inertial and magnetic sensing of human motion", PhD Thesis, University of Twente, Enschede.
- [2] A. Cutti, A. Ferrari, P. Garofalo, M. Raggi, A. Cappello, and A. Ferrari, 2010. 'Outwalk': a protocol for clinical gait analysis based on inertial and magnetic sensors. *Medical and Biological Engineering and Computing*, vol. 48, pp. 17-25.
- [3] J. Chardonens, J. Favre, B. Le Callennec, F. Cuendet, G. Gremion, and K. Aminian, 2011. Automatic measurement of key ski jumping phases and temporal events with a wearable system. *Journal of Sports Sciences*, vol. 30, pp. 53-61.
- [4] H. M. Schepers, E. van Asseldonk, J. H. Buurke, and P. H. Veltink, 2009. Ambulatory Estimation of Center of Mass Displacement During Walking. *Biomedical Engineering, IEEE Transactions on*, vol. 56, p. 1189.
- [5] M. S. Andersen, M. Damsgaard, and J. Rasmussen, 2009. Kinematic analysis of over-determinate biomechanical systems. *Computer Methods in Biomechanics and Biomedical Engineering*, vol. 12, pp. 371-384.
- [6] H. J. Woltring, 1994. 3-D attitude representation of human joints: A standardization proposal. *Journal of Biomechanics*, vol. 27, pp. 1399-1414.

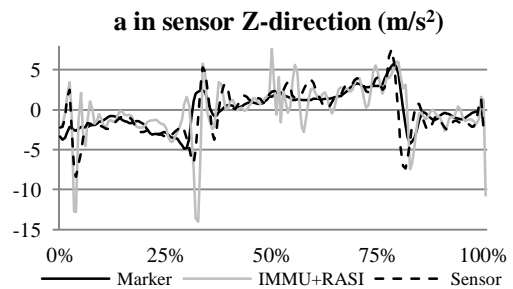


Figure 6 Simulated right thigh sensor net accelerations by subtracting the gravity component in the model IMMU frame for simulations using marker drivers and the IMMU drivers with one marker placed at the right anterior superior iliac spine (RASI) instead of pelvic fixation. The real IMMU net acceleration (Sensor) is calculated by subtracting gravity in the real IMMU frame.